Bound-state effects in $B \to K^*\gamma$

C. E. Carlson
Physics Department, College of William and Mary, Williamsburg, Virginia 23187

J. Milana
Department of Physics, University of Maryland, College Park, Maryland 20742
(Received 16 May 1994; revised manuscript received 7 December 1994)

Applying perturbative QCD methods recently seen to give a good description of the two-body hadronic decays of the B meson, we address the question of bound-state effects on the decay $B \to K^*\gamma$. Consistent with most analyses, we demonstrate that gluonic penguin diagrams, with photonic bremsstrahlung off a quark, change the decay rate by only a few percent. Using an asymptotic distribution amplitude for the K^* and just the standard model we can obtain a branching ratio of a few $\times 10^{-5}$, consistent with the observed rate.

PACS number(s): 13.25.Hw, 12.38.Bx, 14.40.Nd

I. INTRODUCTION

This paper reports on potential bound-state modifications to the analysis of $B \to K^*\gamma$, which is usually given solely in terms of the on-shell subprocess $b \to s\gamma$.

The flavor-changing neutral currents involved in the decays of the B into $K^*\gamma$ do not exist to leading order in the standard model, but can occur in second order in the weak interaction via emission and reabsorption of W bosons [1]. These loop diagrams are often called "penguin" diagrams and their magnitude can be greatly modified by strong interaction effects [2–4].

There is recent further interest in these decays because additional penguinlike contributions could come from particles not in the minimal standard model [5,6]. Contributions to B into $K^*\gamma$ decay from loops of nonstandard-model particles (such as loops of supersymmetric particles) would be a signal of their existence. To take advantage of this possibility, a more precise study of the decay in the standard model needs to be undertaken.

The subprocess $b \to s\gamma$, taken as a free decay, is usually treated as the only flavor-changing contribution leading to $B \to K^*\gamma$ [7]. However, bound-state effects could seriously modify results coming from this assumption. Bound-state effects include modifications involving gluonic penguin diagrams or double (photon plus gluon) penguin diagrams, and contributions from annihilation diagrams. The latter involve no neutral flavor-changing currents at all.

We shall use perturbative QCD (PQCD) in our analysis (see also [8]), a methodology we have previously applied [9,10] to hadronic decays and semileptonic form factors of the B, inspired by Ref. [11]. Examples of the Feynman diagrams we calculate are given in Fig. 1. We require as input the effective vertices that result from the penguin diagram analyses [2–4]. Thereafter our calculations are quite explicit and are detailed below.

A preview of our results is as follows. Diagrams involving the subprocess $b \to s\gamma$ do dominate, and keeping just contributions from the most commonly cited effec-

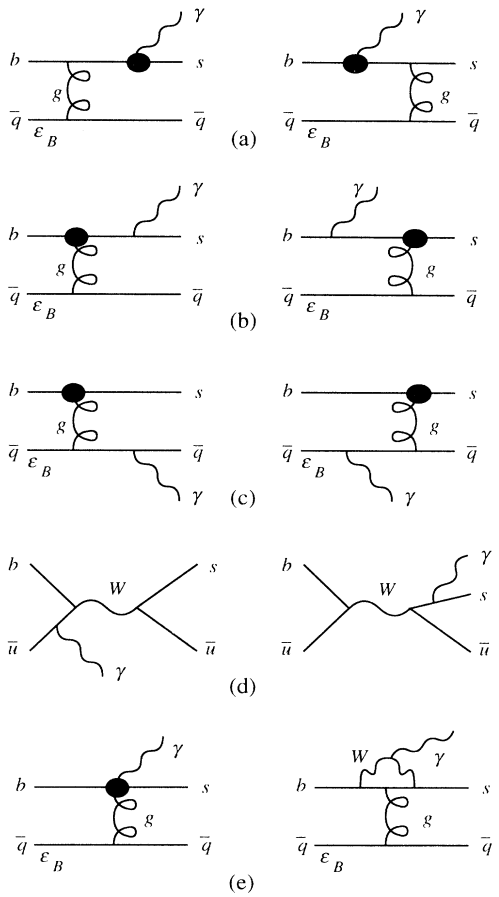

FIG. 1. Diagrams. The effective vertex, due, for example, to a W and t quark loop, is represented as an oval blob; (a) shows the photonic penguin diagrams, (b) shows gluonic penguin diagrams with bremsstrahlung from the b or s quark, (c) shows gluonic penguin diagrams with bremsstrahlung from the spectator quark, (d) shows two of four lowest order annihilation diagrams that could give charged $B \to K^*\gamma$, and (e) shows the "double penguin diagram," once as a blob and once showing one example of a contribution to the blob.

tive vertex gives close to the correct answer. Some cancellation underlies the last statement. Other diagrams involving gluonic penguin diagrams and annihilation are shown to be small, although they lead to a someday measurable few percent difference in the decay rates of the charged and neutral B into $K^*\gamma$ decay.

A diagram we are forced to omit for now is the double penguin diagram, Fig. 1(e), where both a photon and a gluon come out of the loop, as the effective vertex it gives is not calculated.

II. CALCULATIONS

We now begin to describe our calculations in more detail. The penguin diagrams are represented by blobs in Fig. 1, which may be interpreted as an effective Hamiltonian, expanded as

$$H_{\rm eff} = -4\frac{G_F}{\sqrt{2}} V_{tb}V_{ts}^* \sum C_i(\mu) O_i(\mu). \tag{1}$$

The operators O_i are listed in Refs. [2], [3], and [4].

Consider the photonic penguin diagrams in Fig. 1(a). If the incoming and outgoing quarks in $b \to s\gamma$ are on shell, there is only one relevant operator in $H_{\rm eff}$. References [3] contain two operators that can contribute, but using $i\not{D}q = m_q q$ they can be seen to be equivalent. The operator relevant to radiative b decay is then

$$O_7 = \frac{e}{16\pi^2}\, m_b \bar{s}\sigma^{\mu\nu} F_{\mu\nu} \frac{1}{2}(1+\gamma_5)\, b. \tag{2}$$

The notation is that of Ref. [2]; unfortunately, the operator numbering and overall factors of 2 in the definitions do not match among the references.

In the present context, the incoming and outgoing quarks to the penguin transition need not be on shell. It may therefore be instructive to discuss an operator which vanishes for on-shell particles by the equations of motion

$$O_2' = \frac{e}{16\pi^2}\, \bar{s}\sigma^{\mu\nu} F_{\mu\nu} \frac{1}{2}(1+\gamma_5)\,(i\not{D} - m_b)b, \tag{3}$$

where the numbering is from Ref. [3] and the prime reminds us that we have put the on-shell part into the other operator (and that we changed the location of a factor $Q_d = -1/3$). In a perturbative calculation, the inverse propagator piece of O_2' cancels the quark propagator immediately before (after) the penguin transition in Fig. 1(a). The emitted gluon is thereby effectively reduced to being part of the penguin $b \to s\gamma$ transition. From the covariant derivative, O_2' also contains a four-point, contact $b \to s\gamma g$ transition. This additional piece exactly cancels the previous one so that in total O_2' makes no contribution in the present calculation.

We record here the coefficient of O_7 at the W mass scale,

$$C_7(m_W) = \frac{x}{24(1-x)^4}[(1-x)(8x^2+5x-7) + 6x(3x-2)\ln x] = -0.19, \tag{4}$$

where the numerical value is for $x \equiv m_t^2/m_W^2 = 4$, and also record how the operator evolves down to a lower scale:

$$C_7(\mu) = \eta^{-16/3\beta_0}\left[C_7(m_W) - \frac{58}{135}\left(\eta^{10/3\beta_0} - 1\right) - \frac{29}{189}\left(\eta^{28/3\beta_0} - 1\right)\right]. \tag{5}$$

The quantity η is $\alpha_s(\mu)/\alpha_s(m_W)$ and β_0 is $11 - (2/3)n_f$, and following standard practice we have neglected mixing with operators that give small effects. Note that C_7 continuously increases in magnitude with decreasing scale μ.

We make the peaking approximation for ϕ_B, the distribution amplitude of the B meson, wherein

$$\phi_B(x) = \frac{f_B}{2\sqrt{3}}\delta(x_1 - \epsilon_B). \tag{6}$$

The decay constant of the B is f_B and x_1 is the light cone momentum fraction carried by the light quark. The mass of the B is given by $m_B = m_b + \bar{\Lambda}_B$ and $\epsilon_B = \bar{\Lambda}_B/m_B$. For the K^* distribution amplitude, we write

$$\phi_{K^*}(y) = \sqrt{3} f_{K^*} y_1 y_2 \tilde{\phi}_{K^*}(y). \tag{7}$$

The normalization is

$$\int_0^1 dy_1\, \phi_{K^*}(y) = \frac{f_{K^*}}{2\sqrt{3}}, \tag{8}$$

so that $\tilde{\phi}_{K^*}(y)$ is unity for the (super)asymptotic distribution amplitude. We also make the approximation that $m_{K^*} = 0$. The second diagram of Fig. 1(a) is then zero.

The spin projection operators for the initial and final hadronic states are $\gamma_5(\not{p} - m_B)/\sqrt{2}$ and $\not{\xi}^*(\not{k} + (m_{K^*}))/\sqrt{2}$, respectively, with p, k, and q being the momenta of the B, K^*, and photon, and ξ the polarization vector of the K^*. Angular momentum conservation allows only transverse polarizations.

The result is

$$M_{\rm photonic\ penguin} = -\frac{8G}{m_B \epsilon_B} C_7(\mu) I \times \left(p\cdot q \epsilon^* \cdot \xi^* + i\epsilon_{\mu\nu\alpha\beta} p^\mu q^\nu \epsilon^{*\alpha} \xi^{*\beta}\right), \tag{9}$$

where ϵ is the polarization of the photon and

$$G = C_F \frac{e\alpha_s}{4\pi}\frac{G_F}{\sqrt{2}} V_{tb}V_{ts}^* f_B f_{K^*} \tag{10}$$

for $B = u\bar{b}$ decay and requires that the photon and K^* be purely right handed. (For $\bar{B}$ they would be purely left handed.) Also

$$I = (1-\epsilon_B)\int_0^1 dy_1\, \tilde{\phi}_{K^*}(y)\, \frac{(1-y_1)(1+y_1-2\epsilon_B)}{y_1 - 2\epsilon_B - i0^+} \tag{11}$$

$$= (1-\epsilon_B)\left(-\frac{1}{2} + (1-2\epsilon_B)\left[i\pi + \ln\frac{1-2\epsilon_B}{2\epsilon_B}\right]\right), \tag{12}$$

where the integrated result is for the asymptotic distribution amplitude. The imaginary part comes from an internal propagator going on shell. This is often taken as a signal that PQCD is inapplicable. However, if properties of the reaction overall dictate short distance propagation only, then PQCD can still be used [12]. This is the situation here, as discussed in [9] and [13].

Numerical results will be given after we have discussed what prove to be the subdominant contributions. Our understanding of why they are subdominant is helped by some order of magnitude estimates. The crucial expansion parameter is $1/\epsilon_B$ and its logarithms. Factors of ϵ_B come from the propagators, and can also be induced, depending on circumstances, by the factor $y_1 y_2$ in the K^* distribution amplitude.

In the photonic penguin diagrams, Fig. 1(a), the gluon connects at the lower vertex to on-shell quarks and its propagator gives a factor proportional to $1/y_1\epsilon_B$, where y_1 and ϵ_B are the momentum fractions of the two light quarks. Thus appears one factor of $1/\epsilon_B$; the y_1 is canceled from the K^* distribution amplitude. The b quark propagator is involved in two subprocesses: scattering from the light quark by gluon exchange and decay into the s quark plus photon. Both are possible for an on-shell b quark, and the b quark does go on shell in this diagram when $y_1 = 2\epsilon_B$. The b quark propagator thus contributes an imaginary pole term and a real principal value term to the integral involving the K^* distribution amplitude, and one of them gives (roughly speaking) an $i\pi$ and the other gives a logarithm of $1/\epsilon_B$. Now we have accounted for the ϵ_B factors that appear in the photonic penguins diagrams:

$$M_{\text{photonic penguin}} \approx (\text{factors})\frac{1}{\epsilon_B} \times C_7(\mu) \times O\left(i\pi \text{ or } \ln\frac{1}{\epsilon_B}\right). \quad (13)$$

The gluonic penguin graph with emission of the photon from the b or s quark [Fig. 1(b)] does not allow the quark propagator to be on shell. For example, in the diagram with photon emission from the s quark, the internal s quark decaying into an on-shell photon and an on-shell s quark must have a momentum squared larger than the mass squared of the s. A similar argument shows the b propagator is never on shell in the diagram with photon emission from the b quark. The gluon propagator is still spacelike and still gives a $1/\epsilon_B$, but compared to the previous case we lose the $\ln(1/\epsilon_B)$ or $i\pi$ that came from the quark propagator:

$$M_{b \text{ or } s \text{ bremss}} \approx (\text{similar factors}) \times \frac{1}{\epsilon_B} \times C_8(\mu) \times \text{const.} \quad (14)$$

As we shall see, another significant reduction comes from replacing coefficient C_7 by its gluonic counterpart C_8, which we display below.

For the spectator bremsstrahlung case, Fig. 1(c), the quark propagator cannot go on shell. However, the gluon propagator can. A factor $(1/\epsilon_B)$ that came from the gluon propagator is lost, and replaced by factors $i\pi$ or $\ln(1/\epsilon_B)$ that come from integrating the K^* quarks' momentum fraction over the gluon pole, yielding

$$M_{\text{spectator bremss}} \approx (\text{similar factors})(\epsilon_B)^0 \times C_8(\mu) \times O\left(i\pi \text{ or } \ln\frac{1}{\epsilon_B}\right). \quad (15)$$

Thus these gluonic penguin diagrams are suppressed by powers of ϵ_B or logarithms thereof, as well as by the ratio C_8/C_7.

For the actual calculations involving the gluonic penguin diagram we kept just O_8 in the effective Hamiltonian, where

$$O_8 = \frac{g}{16\pi^2}\, m_b \bar{s}\sigma^{\mu\nu} G_{\mu\nu} T_a \frac{1}{2}(1+\gamma_5)\, b. \quad (16)$$

The numbering is that of Ref. [2]. Other operators are possible when the gluon is off shell. We have not explicitly calculated their contributions in this case, but have verified that the order of magnitude estimates are not upset, i.e., they are not leading in $1/\epsilon_B$.

The results are

$$M_{b \text{ or } s \text{ bremss}} = \frac{8 e_d G}{m_B \epsilon_B} C_8(\mu) I' \times \left(p\cdot q \epsilon^*\cdot\xi^* + i\epsilon_{\mu\nu\alpha\beta} p^\mu q^\nu \epsilon^{*\alpha}\xi^{*\beta}\right), \quad (17)$$

where $e_d = -1/3$, G has the same meaning as before, and I' is

$$I' = \int_0^1 dy_1\,(1-y_1)\,\tilde{\phi}_{K^*}(y) = \frac{1}{2}, \quad (18)$$

with the integrated result being for the asymptotic distribution amplitude; and

$$M_{\text{spectator bremss}} = -\frac{4 e_q G}{m_B} C_8(\mu) I_0(\epsilon_B) \times \left(p\cdot q \epsilon^*\cdot\xi^* + i\epsilon_{\mu\nu\alpha\beta} p^\mu q^\nu \epsilon^{*\alpha}\xi^{*\beta}\right), \quad (19)$$

where e_q is the quark charge for the spectator. We neglected some small terms in the numerator and let

$$I_0(\epsilon_B) = -i\pi + \ln\frac{1-\epsilon_B}{\epsilon_B}. \quad (20)$$

The coefficient C_8 is

$$C_8(m_W) = -\frac{x}{8(1-x)^4}\left[(x-1)(x^2-5x-2)+6x\ln x\right] = -0.094, \quad (21)$$

where the numerical value is again for $x = 4$, and it evolves like [4]

$$C_8(\mu) = \eta^{-14/3\beta_0}\left[C_8(m_W) - \frac{151}{288}\left(\eta^{8/3\beta_0}-1\right) + \frac{11}{936}\left(\eta^{26/3\beta_0}-1\right)\right]. \quad (22)$$

Additionally, there are the annihilation graphs,

Fig. 1(d). These can contribute only to $B^{\pm}$ decay. They were considered in the context of D decay some time ago [14], though not for exclusive hadronic final states. Exclusive final states from annihilation diagrams were considered more recently [15] using a nonrelativistic model and a "duality" model. We can here do a relativistic calculation, aided by the fact that to leading order in $(\epsilon_B)^{-1}$ the result comes only from bremsstrahlung off the initial u quark, the first of Fig. 1(d). Part of this graph is just the W turning into a K^* so that part can be evaluated recalling the definition of the decay constant f_{K^*}.

Leading order in $(\epsilon_B)^{-1}$ gives

$$M_{\rm ann} = \frac{2e_u}{m_B \epsilon_B} \frac{m_{K^*}}{m_B} \left[e \frac{G_F}{\sqrt{2}} V_{ub} V_{us}^* f_B f_{K^*} \right] \times \left(p \cdot q \epsilon^* \cdot \xi^* + i \epsilon_{\mu\nu\alpha\beta} p^\mu q^\nu \epsilon^{*\alpha} \xi^{*\beta} \right), \quad (23)$$

where we kept m_{K^*} when it appeared as an overall factor and where $e_u = 2/3$. The quantity in square brackets differs from the quantity G used earlier in lacking the strong interaction factors $C_F \alpha_s / 4\pi$ and in having different Cabibbo-Kobayashi-Maskawa (CKM) factors. While it is interesting that the decay proceeds at all without flavor-changing neutral currents, the result turns out small. Not having the gluon exchange is a plus numerically, but the factors m_{K^*}/m_B and V_{ub} ensure the small result.

III. NUMERICAL RESULTS

The numerical results should not depend on the renormalization scale. However, as we are most familiar with the wave functions or distribution amplitudes at a typical hadronic scale, say $\mu \approx 1$ GeV, we should evaluate the other quantities at the same scale. There are very big changes in the C_i from their values at the W mass scale.

For definiteness we shall use

$$\Lambda_{\rm QCD} = 100 \text{ MeV}, \quad \bar{\Lambda}_B = 500 \text{ MeV},$$

$$m_W = 81 \text{ GeV}, \quad m_t = 2 m_W,$$

$$V_{ts} = -0.045, \quad V_{tb} = 0.999,$$

$$V_{ub} = 0.0045, \quad V_{us} = 0.22,$$

$$\tau_B = 1.46 \text{ ps},$$

$$f_B = 132 \text{ MeV}, \quad \text{and} \quad f_{K^*} = 151 \text{ MeV}.$$

Our convention has $f_\pi = 93$ MeV; the value of f_B is taken from lattice gauge theory [16] and the value of f_{K^*} is got from the measured $\tau \to K^* \nu$ decay rate [17]. The signs of the CKM parameters follow a "standard" advocated in [18]. The sign of $V_{tb} V_{ts}^* / V_{ub} V_{us}^*$ is what is crucial and does not depend on conventions. We use the asymptotic form for the K^* distribution amplitude and will mention results with another form later. We will express each contribution to the amplitude as

$$M_i = t_i \times \frac{1}{2} \left[\epsilon^* \cdot \xi^* + i (p \cdot q)^{-1} \epsilon_{\mu\nu\alpha\beta} p^\mu q^\nu \epsilon^{*\alpha} \xi^{*\beta} \right], \quad (24)$$

whereupon

$$\Gamma = \frac{1}{16 \pi m_B} |t|^2 \quad (25)$$

for t being the sum of the t_i (and neglecting the K^* mass).

The scale we should use should be compatible with the scale that our wave functions and distribution amplitudes are determined at, and this in turn should be consistent with the scale of the four-momentum squared of the off-shell gluon. This suggests $\mu \approx 0.8$ GeV, which we shall use. We extrapolate the coefficients according to the formulas given earlier. Much of the change due to the extrapolation occurs as the scale changes from m_W down to order m_B, at least for the large terms proportional to C_7. For the running coupling we use $\alpha_s = 4\pi / [\beta_0 \ln(\mu^2 / \Lambda_{\rm QCD}^2)]$ with the number of flavors appropriate to the scale.

From operator O_7 we get

$$t_7 = -0.95 - 3.56i. \quad (26)$$

The amplitudes are in units of 10^{-8} GeV. For others we get

$$t_{\text{b or s bremss}} = -0.10,$$
$$t_{\text{spectator bremss}} = -0.04 + 0.06i,$$
$$t_{\rm ann} = 0.06. \quad (27)$$

The last two are given for the charged B. The photonic penguin diagrams dominate, although the other graphs contribute circa 10% corrections to the real parts of the decay amplitude.

In total we get a branching fraction

$$B(B \to K^* \gamma) = 1.13 \times 10^{-5} \quad (28)$$

including just the photonic penguin terms. It seems inconsistent to include the smaller contributions since they may be smaller than the errors induced by our approximations upon the big terms. However, keeping all terms anyway gives 1.11×10^{-5} for the neutral B and 1.16×10^{-5} for the charged B. The relative size of the neutral and charged B decays should be about right and would be interesting to observe when very precise data become available.

It is possible that the distribution amplitude for the transversely polarized K^* is narrower than the asymptotic one. Chernyak, Zhitnitsky, and Zhitnitsky [19] suggested a distribution amplitude

$$\tilde{\phi}_{K^*}(y) = 5 (y_1 y_2)^2, \quad (29)$$

albeit this was for the transverse ρ. If we use this distribution amplitude for the K^*, our calculated branching fractions are almost unchanged (although the phase of t_7 changes noticeably).

The choice of $\Lambda_{\rm QCD}$ was made consistent with some of our own earlier work [9,10], but could be varied (the earlier situation is much less sensitive to the value of this quantity than the present case will prove to be). If we let $\Lambda_{\rm QCD} = 200$ MeV, leaving other parameter choices untouched, the branching ratio with the asymptotic distribution amplitude changes to

$$B(B \to K^*\gamma) = 3.27 \times 10^{-5} \tag{30}$$

including just photonic penguin terms, with commensurate changes in results keeping all terms. These values are in accord with present experimental data [20]. It is also clear that values for other parameters could be varied somewhat from values that we have used.

IV. CONCLUSION

It seems with present knowledge that the actual $B \to K^*\gamma$ decay rate is sensitive to parameters of the bound state and to parameters governing the evolution of QCD. Still, a number of conclusions may be drawn.

The contributions from gluonic penguin and annihilation diagrams, which contribute to the physical decay but not to $b \to s\gamma$, have been calculated here. They change the decay rate by a few percent and so are not worrisome until the experiments are considerably more precise.

Regarding the future, there is a need to calculate the double penguin diagrams mentioned in the Introduction and illustrated in Fig. 1(e), including the QCD corrections to them. For now, we can at least note that in these diagrams the imaginary parts are expected to be at least m_c^2/M_B^2 [21] suppressed so that the imaginary parts already calculated here should remain nearly unaffected and put a lower bound on the total result. Also, one will wish to eventually study the totality of $B \to X_s\gamma$ since this is closer to the basic $b \to s\gamma$ than any individual exclusive channel.

Nonetheless, the opportunity to test the flavor-changing neutral currents induced in the standard model and to search for evidence of particles or phenomena beyond the standard model makes B decay into $K^*\gamma$ and into $X_s\gamma$ interesting, and makes calculations to determine precisely the standard model contributions to these decays a worthwhile and necessary pursuit.

ACKNOWLEDGMENTS

We thank H. J. Lu for many detailed discussions and also S. Dawson, J. Donoghue, W. Marciano, and A. Szczepaniak for helpful conversations. We also thank D. Griegel for his input. This work was supported in part by NSF Grant No. PHY-9306141 and DOE Grant No. DOE-FG02-93ER-40762.

[1] M.A. Shifman, A.I. Vainstein, and V.I. Zakharov, Nucl. Phys. **B120**, 316 (1977); F. Gilman and M.B. Wise, Phys. Rev. D **20**, 2392 (1979); T. Inami and C. S. Lim, Prog. Theor. Phys. **65**, 297 (1981).

[2] B. Grinstein, R. Springer, and M.B. Wise, Nucl. Phys. **B339**, 269 (1990); M. Misiak, Phys. Lett. B **269**, 161 (1991).

[3] R. Grigjanus *et al.*, Phys. Lett. B **213**, 355 (1988); G. Cella *et al.*, *ibid.* **248**, 181 (1990).

[4] M. Ciuchini, E. Franco, G. Martinelli, L. Reina, and L. Silvestrini, Phys. Lett. B **316**, 127 (1993); G. Cella, G. Curci, G. Ricciardi, and A. Viceré, *ibid.* **325**, 227 1994; A. Ali, G. Giudice, and T. Mannel, Report No. CERN-TH.7346/94, 1994 (unpublished), Appendix.

[5] J. Hewitt, Phys. Rev. Lett. **70**, 1045 (1993); V. Barger, M. Berger, and R. Phillips, *ibid.* **70**, 1368 (1993); T. Hayashi, M. Matsuda, and M. Tanimoto, Prog. Theor. Phys. **89**, 1047 (1993).

[6] R. Barbieri and G.F. Giudice, Phys. Lett. B **309**, 86 (1993); R. Garisto and J.N. Ng, *ibid.* **315**, 372 (1993).

[7] This is also true of the lattice gauge calculations, K.C. Bowler *et al.*, Phys. Rev. Lett. **72**, 1398 (1994); C. Bernard, P. Hsieh, and A. Soni, *ibid.* **72**, 1402 (1994).

[8] P.A. Griffin, M. Masip, and M. McGuigan, Phys. Rev. D **50**, 5751 (1994).

[9] C.E. Carlson and J. Milana, Phys. Lett. B **301**, 237 (1993).

[10] C.E. Carlson and J. Milana, Phys. Rev. D **49**, 5908 (1994).

[11] A. Szczepaniak, E.M. Henley, and S.J. Brodsky, Phys. Lett. B **243**, 287 (1990).

[12] S. Coleman and R.E. Norton, Nuovo Cimento **28**, 438 (1965); G. Farrar, G. Sterman, and H. Zhang, Phys. Rev. Lett. **62**, 2229 (1989); R. Kahler and J. Milana, Phys. Rev. D **47**, R3690 (1993).

[13] C.E. Carlson, in Proceedings of the 6th Regional Conference on Mathematical Physics, Islamabad, Pakistan, 1994 (unpublished).

[14] M. Bander, D. Silverman, and A. Soni, Phys. Rev. Lett. **44**, 7 (1980).

[15] D. Atwood and A. Soni, Z. Phys. C **64**, 241 (1994).

[16] C.W. Bernard, J.N. Labrenz, and A. Soni, Phys. Rev. D **49**, 2536 (1994).

[17] P. Colangelo, C.A. Dominguez, G. Nardulli, and N. Paver, Phys. Lett. B **317**, 183 (1993).

[18] Particle Data Group, K. Hikasa *et al.*, Phys. Rev. D **45**, S1 (1992), I.1.

[19] V. Chernyak, A. Zhitnitsky, and I. Zhitnitsky, Nucl. Phys. **B204**, 477 (1982).

[20] CLEO Collaboration, R. Ammar *et al.*, Phys. Rev. Lett. **71**, 674 (1993). They give branching fraction $(4.5 \pm 1.5 \pm 0.9) \times 10^{-5}$ and see both B^0 and B^-.

[21] A. Ali and C. Greub, Z. Phys. C **49**, 431 (1991).